Effect of temperature sensitive ion channels on the single and multilayer network behavior of an excitable media with electromagnetic induction

Anitha Karthikeyan

Electronics and Communication Engineering, Prathyusha Engineering College, Chennai, India.

mrs.anithakarthikeyan@gmail.com

Irene Moroz

Mathematical Institute, University of Oxford, Andrew Wiles Building, Oxford, UK.
irene.Moroz@maths.ox.ac.uk

Karthikeyan Rajagopal

Center for Nonlinear Systems, Chennai Institute of Technology, India.

karthikeyan.rajagopal@citchennai.net; rkarthiekeyan@gmail.com

Prakash Duraisamy

Center for Nonlinear Dynamics and Control, Mekelle University, Ethiopia.
duraiprakash83@gmail.com

Abstract

The dynamical behavior of the neurons directly depends on the transition from resting to spiking states. These transitions show different types of bifurcations and has different spiking periods. The transitions are also affected by the temperature exposure of the ionic channels. To understand such effects, we investigate the Morris-Lecar (ML) neuron model with temperature affected calcium, potassium and leak current channels. The presented ML model is considered with electromagnetic field coupling considering a simple cubic memristor flux relation. Firstly the basic dynamical properties of the ML model is analyzed considering the current temperature as the control parameter. The temperature affected ionic channels in the ML model leads to various types of oscillations from periodic spiking to chaotic bursting. These bifurcation patterns are well discussed with corresponding Lyapunov exponents. To study the wave propagation in the temperature dependent ML model (TDML), we have constructed two different types of network structure. In the first a simple lattice network is considered with the local nodes of the TDML neurons and the temperature effects on the wave propagation is studied individually for the three channels. In the second type of network, we have considered inter coupled three lattice layers of TDML neurons. This discussion is subdivided in to two cases and in the first case the layers are constructed such that the first, second and third layers having temperature affected calcium, potassium and leaky current channels respectively. In the second case we considered only one channel to have temperature effects and the others have no temperature affected ion channels. The wave

propagation phenomenon in both the types of network is analyzed considering the current temperature as the control parameter.

Keywords: Morris-Lecar model; temperature effects; bifurcation; multilayer; spiral waves;

1. Introduction

Neuronal activities such as signaling process within and among cells been modeled with numerous mathematical models. Models based on the charged particles which is interacting the potential of the neuron are widely used for analyzing the network dynamics of neuron. Quiescence, Spiking and Bursting are the various dynamical behaviors identified in the real neurons. Morris–Leccar (M-L) model can efficiently expose such complex behaviors and proved that it is compatible for simulations. Presence of electromagnetic induction influences much in mode transition in electrical activities of neuron dynamics [1, 2-4]. Hence electrical activity patterns of neurons can be easily controlled by tuning the external magnetic field parameters, which includes spiking state, bursting state, periodic state and even chaotic state. Electromagnetic radiation can improve the synchronization degree of negative feedback coupled neurons meanwhile manage the discharge of positive feedback couple neurons [5, 6]. Because of the advantages of mimicking various real-time behaviors particularly network dynamics, it is obvious to get interested to investigate the M-L model with electromagnetic induction.

Different conditions and channel types can be regulated by altering temperature and this complex set of changes may lead to unpredictable effects on neuronal behaviors [7–9]. Experimental investigation discussed in [10] revealed that the influence of temperature in properties such as synaptic inputs, active conductance and passive membrane potential has significant effect. We couldn't find much literature to replicate and simulate such behaviors using mathematical model except [11]. The effects of temperature on the action potential of neuron investigated and numerical computations are carried out using H-H model with electromagnetic induction. The study focused only with fixed condition of electromagnetic induction. The challenge identified in the study for investigating network behavior is the complexity of the equations used in Hodgkin-Huxley (H-H) model. From this discussion, we can easily understand the significance of M-L model, which expose most of the properties and can support better for simulation. More importantly, investigating the neuron behavior collectively can provide real-time results rather single neuron consideration. Nonlinear behaviors of neurons varied based on the appropriate distribution of autopse in the network [12,13], the positive and negative feedback in autapse can persuade significant effect on wave propagation [14-16].

Motivated from the above discussion in this paper we considered M-L model with electromagnetic induction for studying the influence of temperature effects focusing on network dynamics. We presented the temperature-sensitive ML model and subdivided the discussions into three cases as depending on the temperature affected ion channels. We discussed linear stability analysis in the following section. We carried out bifurcation analysis and provided the bifurcation diagrams and corresponding Lyapunov spectrum. The major contribution of this paper is investigating Spatiotemporal behavior of the Temperature-

sensitive ML model. Network dynamics of a multilayer network also discussed. Finally concluding remarks with proper interpretation also provided.

2. Temperature sensitive ML model:

In order to investigate the temperature effects on the ion channels, we consider the modified Morris-Lecar neuron model [18] proposed in [17] defined by three differential equations as

$$\begin{aligned} C\dot{V} &= g_{CaT} M_{\infty}(V_{Ca}-V) + g_{KT} W(V_K - V) + g_{¿}(V_L - V) - I \\ \dot{W} &= \tau_{WT}(W_{\infty} - W) \\ \dot{I} &= \varepsilon(V_0 + V) \end{aligned} \qquad (1)$$

In the above model, V and W are the membrane potential and the gate probability of potassium channels respectively and I, represents the slow bursting variable. The most important modification in the above model is the inclusion of the temperature effects on the ion channels. To model this effect, we define the following relations inspired by the discussions in [17],

$$\begin{aligned} g_{CaT} &= g_{Ca} Q_{Ca}^{TE} \\ g_{KT} &= g_K Q_K^{TE} \\ g_{¿} &= g_L Q_L^{TE} \\ \tau_{WT} &= \tau_W Q_w^{TE} \end{aligned} \qquad (2)$$

where $TE = (T_c - T_r)/10$ is the temperature effect on the respective channels with T_c representing the current temperature and T_r, the reference temperature. The parameters g_{Ca} and g_K are the total conductance values for all calcium and potassium while g_L is the leak conductance value and the parameter Q denotes the temperature sensitivity constant. The other system parameters V_{Ca}, V_K, and V_L are the steady-state Nernst potentials of calcium ions, potassium ions, and leak channels, respectively. The three special functions $M_{\infty}, W_{\infty}, \tau_W$ representing the opening probability for all calcium, and potassium channels and time constant of the potassium activation respectively are defined by ,

$$\begin{aligned} M_{\infty} &= 0.5 + 0.5 \tanh\left(\frac{V - V_1}{V_2}\right) \\ W_{\infty} &= 0.5 + 0.5 \tanh\left(\frac{V - V_3}{V_4}\right) \end{aligned} \qquad (3)$$

$\tau_W = \sigma^{-1}\cosh 0.5\left(\frac{V-V_3}{V_4}\right)$	

Many literatures have shown that the electromagnetic induction [19-22] can introduce complex effects in a neuron model and recently in [23], the authors have shown that by including electromagnetic effects in the M-L neuron model we can explore complex dynamics including the chaotic behavior. Hence, we introduce the modified temperature depended extended M-L model (TDML) with electromagnetic induction as

$C\dot{V} = g_{CaT} M_\infty (V_{Ca} - V) + g_{KT} W (V_K - V) + g_{¿} (V_L - V) - I - k_0 M(\phi) V = F$ $\dot{W} = \tau_{WT}(W_\infty - W) = \mathrm{G}$ $\dot{I} = \varepsilon (V_0 + V) = \mathrm{H}$ $\dot{\phi} = k_1 V - k_2 \phi = \mathrm{R}$	(4)

where $M(\phi) = \alpha + 3\beta\phi^2$ is the electromagnetic effect on the neuron with ϕ denoting the magnetic flux for the neuron. Such electromagnetic induction is to replicate the effect of moving charges which will induce a magnetic field and magnetic coupling will trigger and modulate the phase synchronization between two identical neurons connected by electric synapse [24]. For the numerical analysis we have used the system parameters as in [23] with the reference temperature fixed as T_r =22. In our entire discussion we have considered the current temperature (T_c ¿ as the control parameter. We have subdivided the discussions in to three cases as depending on the temperature affected ion channels as,

Case-a: Temperature sensitive Calcium ion channels (without and with magnetic induction)
Case-b: Temperature sensitive Potassium ion channels (without and with magnetic induction)
Case-c: Temperature effects on the leak current (without and with magnetic induction)

By properly choosing the scaling factor $Q_i^{TE}, i \in (Ca, K, L, w)$ we can introduce temperature effects in the respective channels. For case-a, we consider $Q_{Ca}=3$ while the other scaling factors are unity. Similarly, for case-b and case c we consider $Q_K=3$ and $Q_L=3$ respectively. This scaling definitions are taken after the ref. [17].

3. Numerical analysis:

3.1 Equilibrium points and stability analysis:

The linear stability analysis is very similar to that found in a previous study of the extended Morris-Lecar neuron model with electromagnetic induction (Rajagopal et al (2020), in which temperature effects are not considered. The fixed points of eqn (4) are obtained by setting the time derivatives to zero, so that

$V_c = -V_0,$ $W_c = W_\infty,$ $\phi_c = \frac{-k_1 V_0}{k_2},$ $I_c = g_{caT} M_\infty (V_{ca} - V) + g_{KT} W (V_K - V_c) + g_{LT} (V_L - V_c) - k_0 M(\phi) V_c.$	(5)

There is therefore only one fixed point, whose linear stability is found by computing the eigenvalues of the fourth order Jacobian matrix, evaluated at the fixed point.

The characteristic equation $\det(J_c - \lambda I_4) = 0$ becomes:

$\lambda^4 + A_3\lambda^3 + A_2\lambda^2 + A_1\lambda + A_0 = 0$	(6)

where

$A_3 = -(F_V + G_W + R_\varphi),$ $A_2 = F_V(G_W + R_\varphi) + G_W R_\varphi - (G_V F_W + F_I H_V + F_\varphi R_V),$ $A_1 = R_\varphi(G_V F_W - F_V G_W) + F_I H_V (G_W + R_\varphi) + G_W F_\varphi R_V,$ $A_0 = -F_I H_V G_W R_\varphi$	(7)

From eqn (6), we see that a steady state bifurcation ($\lambda = 0$) occurs when $A_0 = 0$ i.e. when

$A_0 = -F_I H_V G_W R_\varphi = \varepsilon \tau_\infty k_2 = 0$	(8)

Where, $k_2 = 0$.

For a Hopf bifurcation, we substitute $\lambda = i\omega$ into eqn(8) to get ω as a common root of

$\omega^4 - A_2\omega^2 + A_0 = 0,$ $\omega^2 = \frac{A_1}{A_3}$	(9)

so that

$A_1^2 - A_1 A_2 A_3 + A_0 A_3^2 = 0$	(10)

In case A, the Hopf bifurcation occurs for $T_c = 17.94$ for $k_0 = 0.8$ and at $T_c = 16.94$ for $k_0 = 0$; for case B, this occurs at $T_c = 33.03$ for $k_0 = 0.5$ and at $T_c = 33.69$ for $k_0 = 0.8$; for case C the Hopf bifurcation occurs when $T_c = 28.03$ for $k_0 = 0.5$ and when $T_c = 28.49$ for $k_0 = 0$.

3.2 Bifurcation and Lyapunov exponents:

We now investigate the nonlinear dynamics by producing bifurcation transition plots as T_c varies for each of the three cases and two subcases.

3.2.1 Case-a: Temperature sensitive Calcium ion channels (without and with magnetic induction)

In order to analyze effect of temperature, the bifurcation diagram is derived and presented in figure 1. The control parameter, current temperature (T_c) is varied for the range $19 \leq T_c \leq 23$. In figure 1(a) describes the various oscillations of the system without electromagnetic induction considering temperature dependent Calcium channels. The initial condition taken for the first iteration is [0,0,0], and reinitialized to the state end values in every iteration. Run time is set to 500 and the parameter range is considered with 4000 divisions. The bifurcation diagram shows periodic, period doubling oscillations route to chaos and period halving exit. Figure 2(a) represents the first two Lyapunov spectrum. We used Wolf's Algorithm [34] to calculate the LE's. Points above the zero line shows positive Lyapunov Exponents and confirms the existence of chaotic oscillations. We could observe that the parameter value till 21.25, the system response doesn't show any chaotic region. During 21.25 to 22.30 packs of chaotic regions are observed.

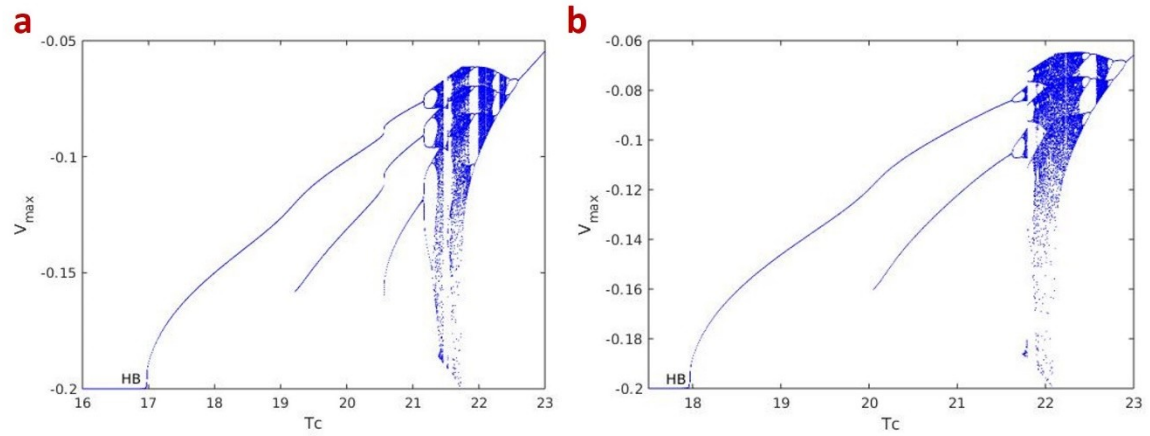

Fig.1a: Bifurcation transition plot of V_{max} as T_c increases for case A for $k_0 = 0$. The Hopf bifurcation is now at $T_c \approx 16.94$. Fig.1b: Bifurcation transition plot of V_{max} as T_c increases for case A and $k_0 = 0.8$. The Hopf bifurcation at $T_c \approx 17.94$ is clearly visible on the T_c axis.

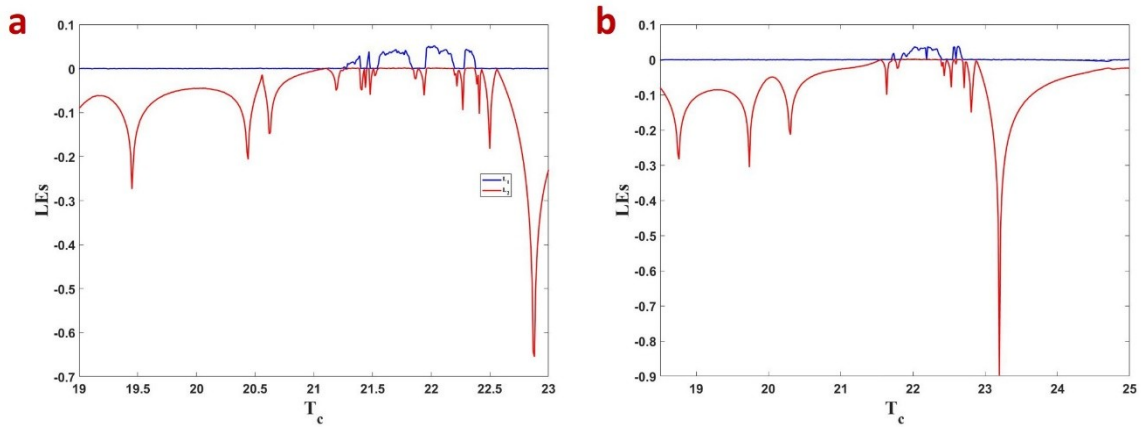

Fig.2a,2b: The corresponding Lyapunov exponents (LEs) calculated for the bifurcation plot shown in Fig.1a and Fig.1b

Figure 1(b) and Figure 2(b) are generated for TDML neuron model with electromagnetic induction. In Figure 1(b) multi periodic oscillations and cascading chaotic regions are observed. Figure 1(d) is the corresponding Lyapunov spectrum. We could observe during the parameter value 20.80 to 22.10, positive Lyapunov exponents. After 22.25 the response of the system is purely periodic oscillation.

3.2.2 Case-b: Temperature sensitive Potassium ion channels (without and with magnetic induction)

The Bifurcation diagrams 3(a) and 3(a) represents the temperature sensitive potassium ion channels without and with magnetic induction respectively. Figure 3(b) and 3(b) are the corresponding Lyapunov spectrums. The parameter current temperature (T_c) is taken in horizontal axis and varied from 19 to 30. The local maximum value of the state variable (V) is taken in the vertical axis. We used Runge-Kutta method to perform numerical simulations and Wolf's Algorithm [34] for calculating Lyapunov Exponents. During this case we considered the temperature sensitivity scaling factor is fixed as [Q_Ca=1;Q_K=3;Q_L=1;Q_w=1]. The bifurcation diagrams explains where the the system response is periodic oscillations and period doubling route to chaos. Period halving exit also observed after the parameter value reaches 24. Bunch of chaotic regions are observed seperated with periodic and period doubling responses.

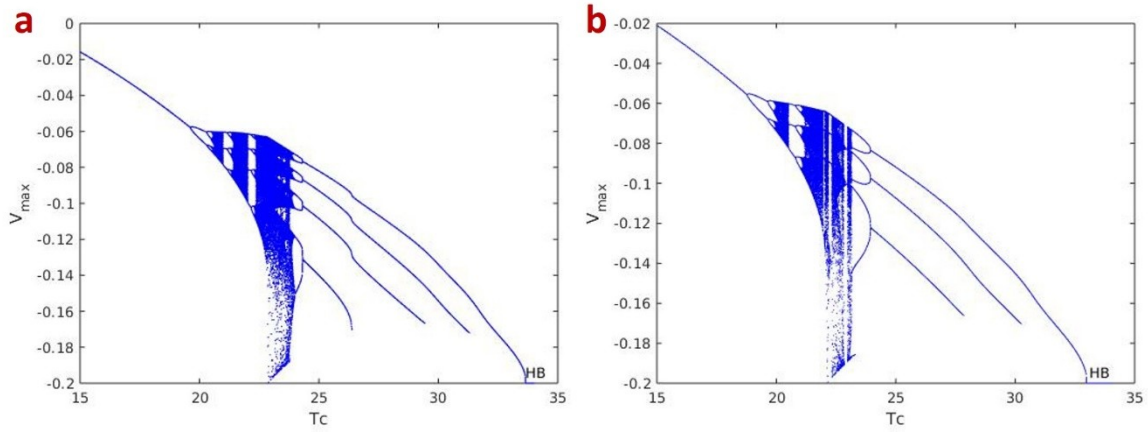

Fig.3a:Bifurcation transition plot of V_{max} as T_c increases for case B for $k_0 = 0$. The Hopf bifurcation is now at $T_c \approx 33.69$. Fig.3b:Bifurcation transition plot of V_{max} as T_c increases for case B for $k_0 = 0.5$ .The Hopf bifurcation is now at $T_c \approx 33.03$.

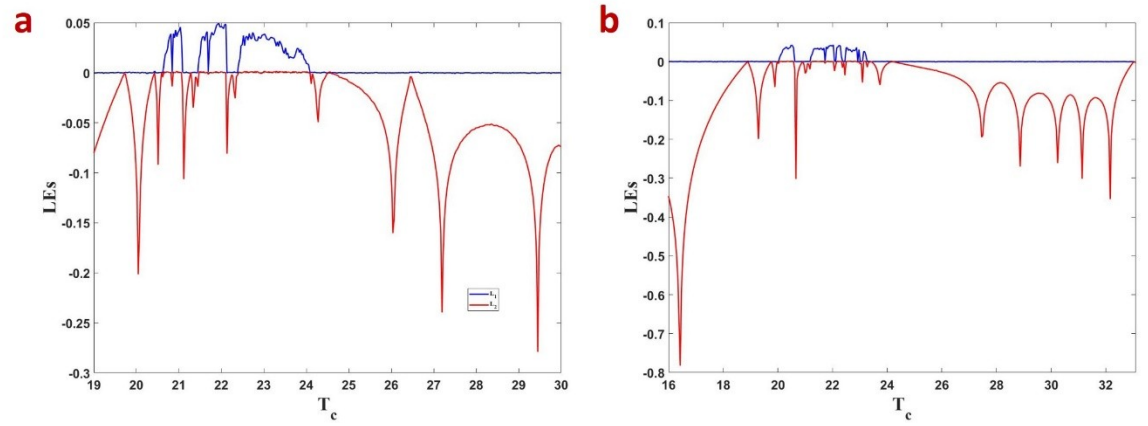

Fig.4a,4b: The corresponding Lyapunov exponents (LEs) calculated for the bifurcation plot shown in Fig.3a and Fig.3b

3.2.3 Case-c: Temperature effects on the leak current (without and with magnetic induction)

TDML neuron model is investigated for the temperature variation on the leak current without and with electromagnetic induction. Figures 5(a) and 5(b) represents the bifurcation diagrams, and figures 3(b) and 3(d) represents first two Lyapunov spectrums. The response of the system for the discussed parameter range shows periodic, period doubling, chaotic and period halving exit. The chaotic regions can be identified with the help of Lyapunov spectrum, where ever the curve crosses the zero line, the system enters into chaotic behavior. We could observe cascade of chaotic regions.

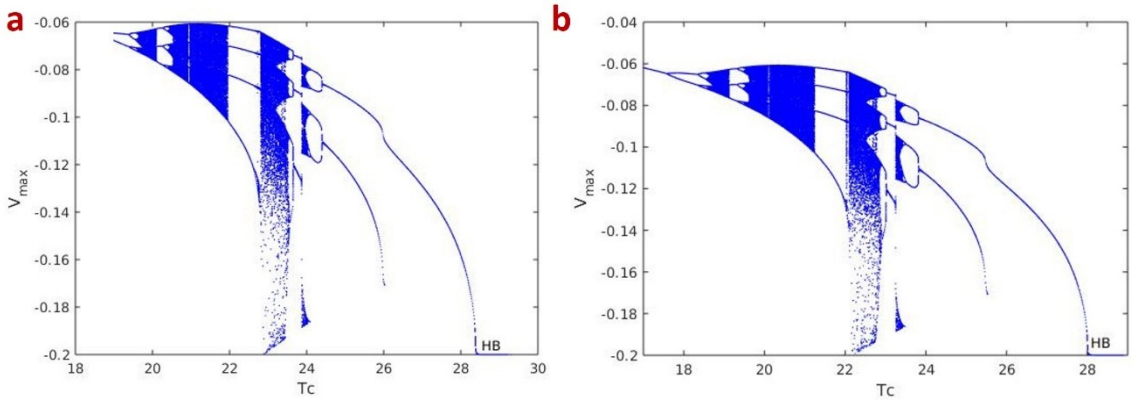

Fig.5a:Bifurcation transition plot of V_{max} as T_c increases for case C for $k_0 = 0$. The Hopf bifurcation is now at $T_c \approx 28.49$. Fig.5b:Bifurcation transition plot of V_{max} as T_c increases for case C and $k_0 = 0.5$. The Hopf bifurcation at $T_c \approx 28.03$ is clearly visible.

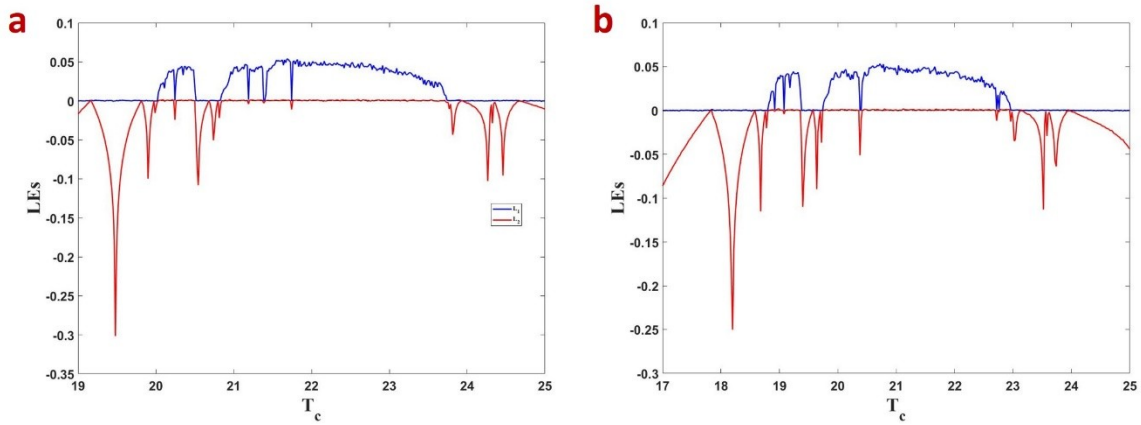

Fig.6a,6b: The corresponding Lyapunov exponents (LEs) calculated for the bifurcation plot shown in Fig.5a and Fig.5b

4. Spatiotemporal behavior of the TDML neurons:

Investigating the spatiotemporal behavior of neurons are important as such discussions will help us to understand some dangerous phenomenon like the spiral turbulence. Some electrical waves in heart are analogous to nonlinear waves exhibited by excitable circuits. In biological conditions, these electrical waves are the reason for the spiral waves seen in heart which results in cardiac arrhythmias leading to sudden cardiac arrest [25]. Some medical studies in the spiral waves in heart tissue has shown their dangerous effects leading to the ventricular fibrillation (VF) [26,27]. Many neuron models exhibit these complex wave patterns when excited with external stimuli forces [28-30]. Some literatures have also showed that using electromagnetic induction and external stimuli, we can suppress these dangerous spiral waves [28,29]. Even though these literatures have discussed about various neuron models, less has been discussions on the spatiotemporal dynamics of neurons with temperature affected ion

channels. As this paper deals with a Morris-Lecar model with electromagnetic induction and temperature affected ion channels, we wish to investigate its network dynamics too.

To study the network behavior of the TDML neurons, we have considered two types of network, In the first network structure, the neurons are arranged in a single layer lattice and in the second network, we have considered a three-layer lattice network. Further its subdivided in each category as TDML without and with electromagnetic induction. The size of the network in both the cases are 110x110 and the external stimuli is $Acos(\omega t)$ whose amplitude is fixed as A=0.1 and frequency as $\omega=0.05$. This stimulus is applied from the left boundary of the network and we have assumed no flux boundary conditions. The local dynamics of the nodes are governed by the TDML neuron whose temperature setting are varied as explained in the sections. The parameters are used as in [7], and we have considered the current temperature T_c as the control parameter.

4.1 Spiral waves in a lattice network of excitable media:

In this section our aim is to investigate the spatiotemporal behavior of a lattice network of excitable media. For this we mathematically modelled the network with 110x110 nodes with each node's dynamics modelled using the TDML neuron. We have used a simulation time of 1000s and the solver used for numerical simulations is the well-known RK4 method with an integration step size fixed as h=0.02. The constructed network is defined as,

$$C\dot{V}_{ij}=g_{CaT}M_{\infty}(V_{Ca}-V_{ij})+g_{KT}W(V_K-V_{ij})+g_{¿}(V_L-V_{ij})-I_{ij}-k_0M(\phi_{ij})V_{ij}+F($$
$$\dot{W}_{ij}=\tau_{WT}(W_{\infty}-W_{ij})\dot{I}_{ij}=\varepsilon(V_0+V_{ij})\dot{\phi}_{ij}=k_1V_{ij}-k_2\phi_{ij} \quad (5)$$

The nearest neighbor coupling function is defined as $F(V_{ij})=D(V_{i+1\,j}+V_{i-1\,j}+V_{ij+1}+V_{ij-1}-4V_{ij})$ with D being the diffusion coefficient. The system parameters used are from [7] with additional parameters Q_{Ca},Q_K,Q_L,Q_w chosen as per the case discussions with $T_r=22$ and the current temperature is considered as the control parameter and the entire analysis is for different values of the temperature T_c with the coupling coefficient fixed at D=1. The stimulus $\varnothing(t)$ is applied to the network in the left boundary and this is achieved using the conditions $\delta_{i\theta_1}=1,\delta_{j\theta_2}=1$ which is true when $i=100,j=0$.

4.1.1 Case-a: Temperature sensitive Calcium ion channels:

We first considered that the Calcium ion channels are affected with the temperature and the settings for the sensitivity constant is $Q_{Ca}=3,Q_K=Q_L=Q_w=1$.This section is subdivided in to two networks scenarios whose node dynamics if governed by TDML without magnetic coupling (scenario-1) and with magnetic coupling (scenario-2). In both the scenarios we have captured the snapshots of the network for different values of the current temperature. For the first scenario the TDML is a three-dimensional system ($k_0=0$¿ and this model is used as the nodes in the network. Fig.4 shows the captured snapshots and we selected six temperature values with reference to the bifurcation plot shown in Fig.7 such that we could cover both periodic spiking and chaotic bursting regions. In the quiescent region ($T_c=21.5$), the applied

stimuli force doesn't induce any spiral waves rather the network shows a quasi-stable target wave which is propagating from the left boundary towards the right but loses the energy before crossing the right boundary. Now when the temperature increases to $T_c=21.8$, the nodes enter chaotic bursting state. This means that the nodes are in random oscillations and several areas of the media goes in to a heterogeneity state thus creating stable spiral waves. As this inhomogeneous media area are due to the node's oscillations in chaotic regime, spiral waves are seen for the temperature regions $21.8 \leq T_c \leq 22.3$. When the local nodes reenter periodic spiking region for $T_c=22.5$, the network media is still in complete heterogeneity ensuring multiple spiral seeds which are slowly seen disintegrated when $T_c \geq 22.8$.

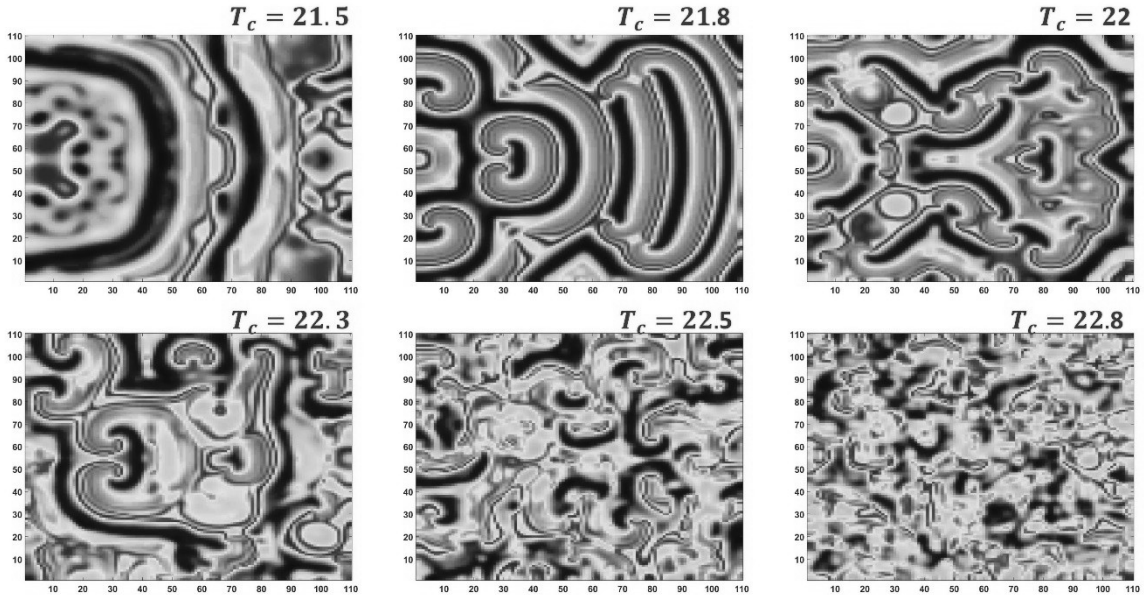

Fig.7: Network snapshots considering temperature affected calcium ion channels in TDML model without electromagnetic field coupling

In the second scenario we have considered the magnetic flux coupling between the neurons with temperature affected calcium channels. Now the nodes are modelled with a four-dimensional TDML neuron and like Fig.7 the temperature effects on the network dynamics are investigated. We again choose the temperature values in accordance with Fig.1b to cover the periodic and chaotic regions. In the periodic regions ($T_c=21.5$¿ when the nodes exhibit spiking the network is in s state of homogeneity and hence the waves are propagated from left to right boundary. Due to the magnetic coupling the neurons close to the left boundary are largely dissipating the stimuli force and thus the spiral waves seen in Fig.3 for $T_c=21.8$ was dissipated in the Fig.4 while a single travelling spiral seed is seen. But when $T_c=22$, the TDML model becomes a simple ML neuron model discussed in [23] and thus shows multiple spiral seeds with several seeds with larger amplitudes. By increasing the temperature, the spiral waves keep disintegrating in to small spiral pools which are gradually lost in the excitable media.

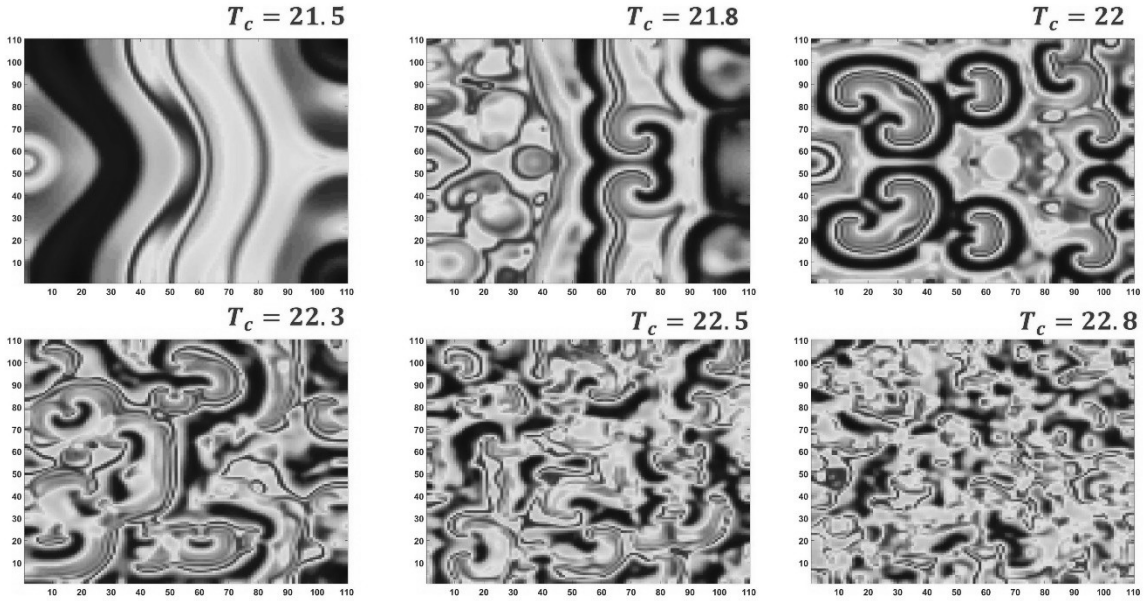

Fig.8: Network snapshots considering temperature affected calcium ion channels in TDML model with electromagnetic field coupling

4.1.2 Case-b: Temperature sensitive Potassium ion channels:

Temperatures in the range of $15\,℃ - 30\,℃$, will affect the potassium channels with irregular firing activities with sudden short period quiescent like states shown in low temperatures whose period keeps increasing as the temperature increases. In other words, the width of the action potential width is more in cold temperatures, the after-hyperpolarization amplitude keeps decreasing with decreasing temperatures. Cell membrane input resistance was higher at lower temperatures [31]. Hence, we are interested to investigate the network dynamics of the TDML model with temperature affected potassium channel. Firstly, comparing Fig.8 and Fig.9 we could say that the temperature range which affect the wave propagation in much larger in case-b compared to case-a. This is because the potassium channels are more as at higher temperatures second messenger gated potassium channels [32] are observed when the $T_c > T_r$.Because of these secondary channels, when the current temperature becomes higher than the reference temperature, we could note the existence of more stable spiral waves in the network. To be noted is that these spiral waves are not propagating type but rotating type which confirms that these are due to the secondary channels opening in particular neurons in the network. Also, these extended rotating spiral waves ($T_c > T_r$¿ are considered to be more dangerous than the propagating spiral waves when $T_c < T_r$ because the rotating spiral wave suppression is more complex [27].

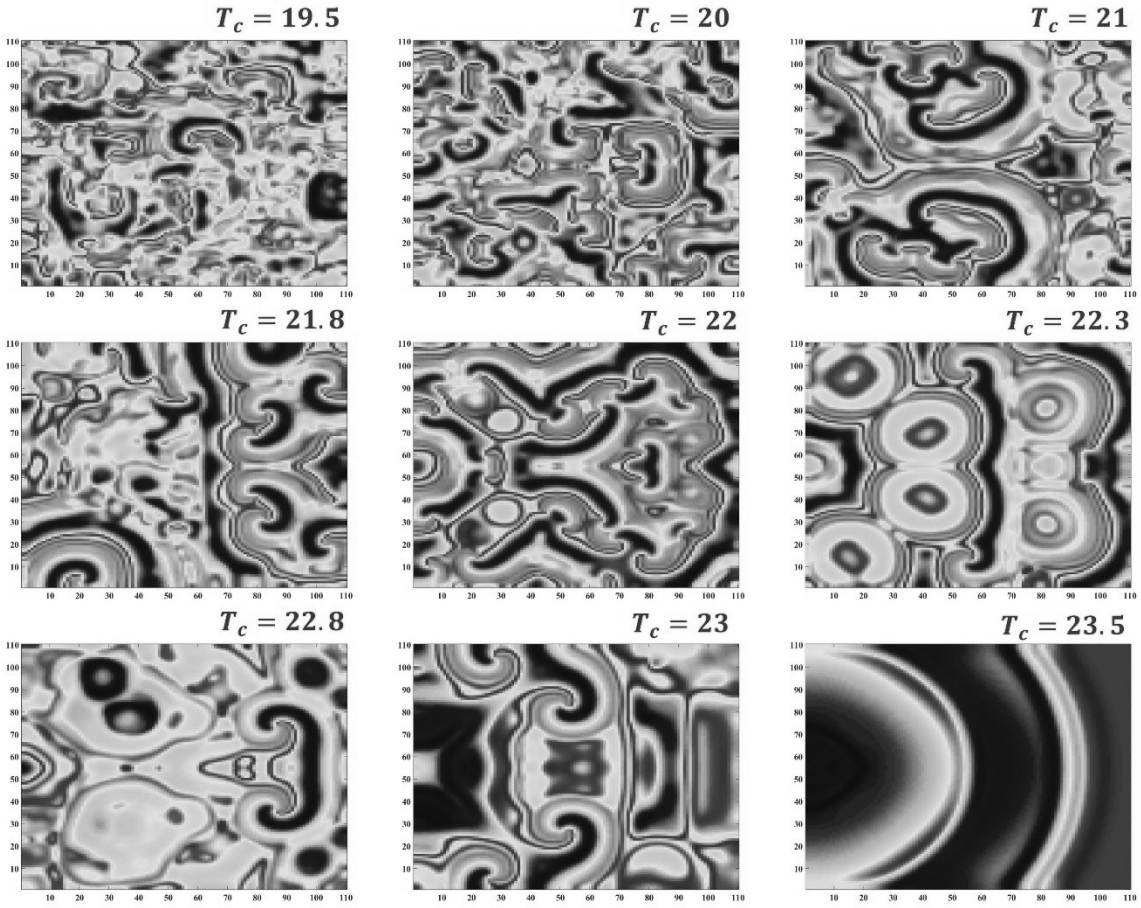

Fig.9: Network snapshots considering temperature affected potassium ion channels in TDML model without electromagnetic field coupling

Many literatures have discussed the effect of magnetic coupling on spiral waves [20,21,28-30] and some have shown that the electromagnetic flux coupling can effectively suppress the spiral waves [33]. Hence, we consider the TDML model with electromagnetic coupling and consider them as individual node in the network (5). We capture the spatiotemporal dynamics of the network for various values of the current temperature as shown in Fig.1. Considering the coupling parameter k_0=0.05, we could see that the range of temperature (T_c¿ showing spiral waves have reduced compared to Fig.9. To be precise, when T_c>$T_r$the spiral waves are suppressed as seen in Fig.14 for T_c=22.5. This confirms that the secondary potassium channels opened due to the temperature effects are now reduced. But increasing the flux coupling strength more than k_0>0.1, results in unstable nodes in the network which in turn makes the entire node unstable.

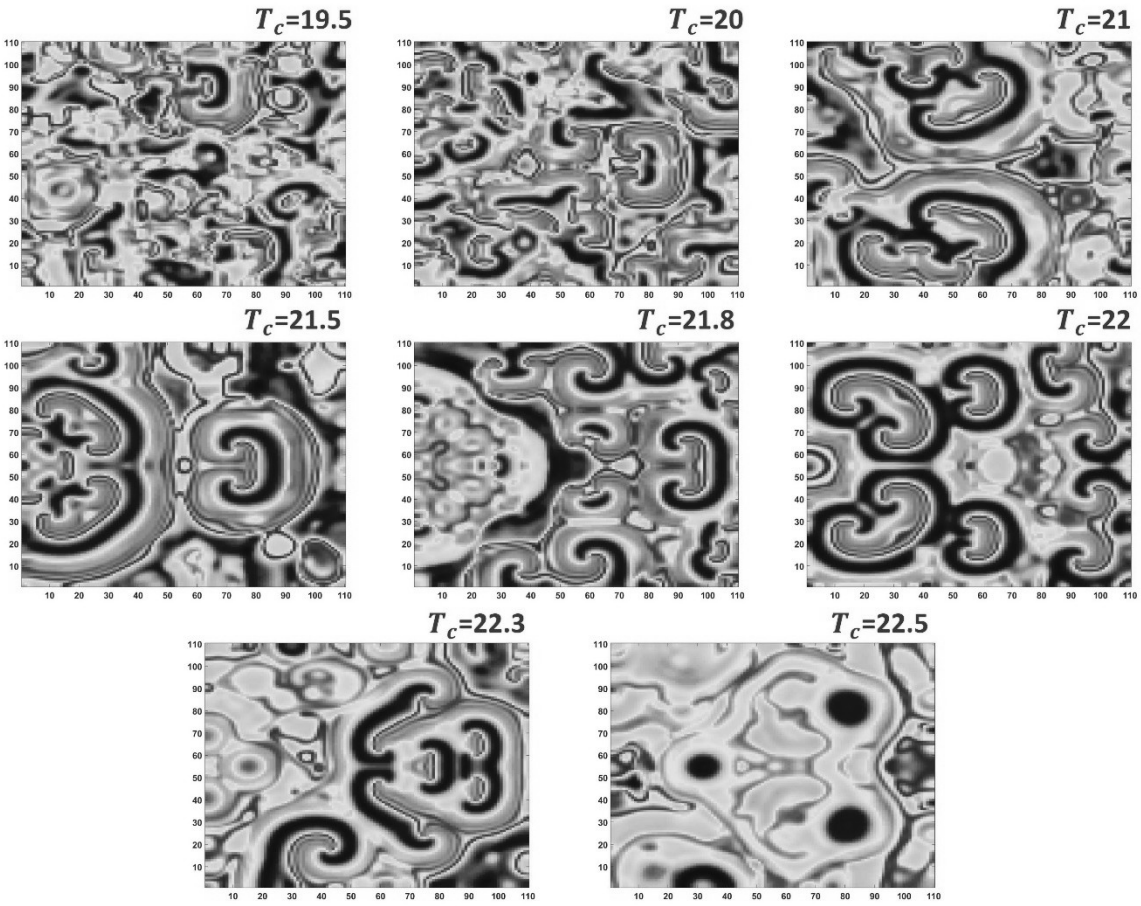

Fig.10: Network snapshots considering temperature affected potassium ion channels in TDML model with electromagnetic field coupling

4.1.3 Case-c: Temperature effects on the leak current:

It was shown in [17] that when temperature effects are considered in the leak current channel, the model changes between class-1 spiking to class-II and then back to class-I depending on the temperature values. But in [17], the authors have considered a simple two-dimensional ML model and, in this work, we have considered a modified version of ML model to accommodate a slow changing variable. For any temperature values $T_c < 20$, the network is completely asynchronous and doesn't have any signs of spiral seeds of target waves. At $T_c = 20$, some nodes try to synchronize with the stimuli settings and thus show initial spiral seeds and by increasing the temperature the spiral seeds are developed to spiral pools due to the increased node synchronization along with the input stimuli. At $T_c = 21.8$ irrespective of which channel is affected by temperature, the network shows spiral waves with much larger radius of rotation and which are much stable even for longer simulation times (10000s). In Fig.11 we have shown the snapshots for 2000s and similar to Fig.9, we could see that the range of temperatures for which the network shows spiral wave turbulence is $20 \le T_c \le 23$ which is wider range compared to Fig.7 showing temperature affected calcium channels.

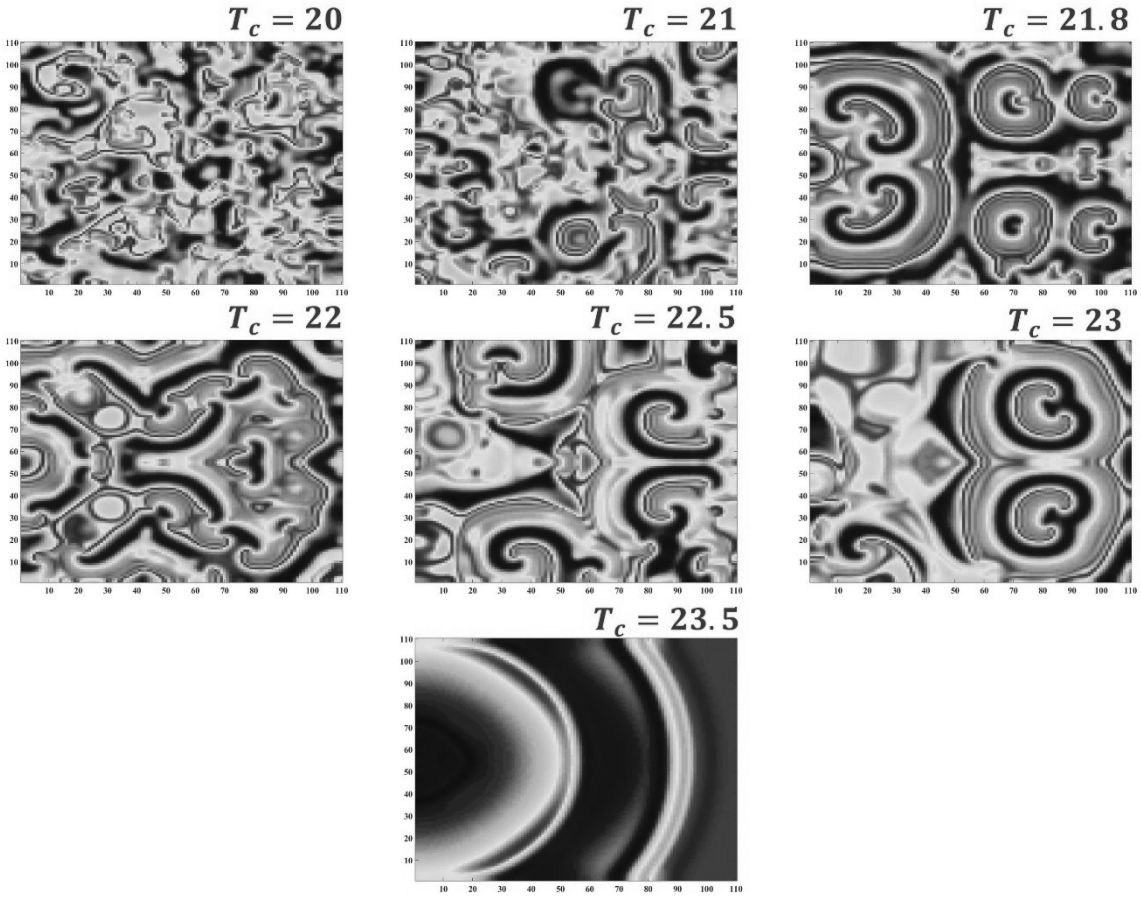

Fig.11: Network snapshots considering temperature affected leaky current in TDML model without electromagnetic field coupling

In this final discussion of this section we include the magnetic flux coupling to the TDML model whose leak current channels are affected by temperature. The network is now constructed with these nodes and a stimulus is applied to the left boundary and the snapshots are captured and shown in Fig.12. We have tried the flux coupling constant values in the range $0.001 \leq k_0 < 0.1$, but couldn't find the value which could effectively eliminate the spiral waves. The network behaved nearly in the same way for the range mentioned and we have presented the snapshots for $k_0 = 0.05$.

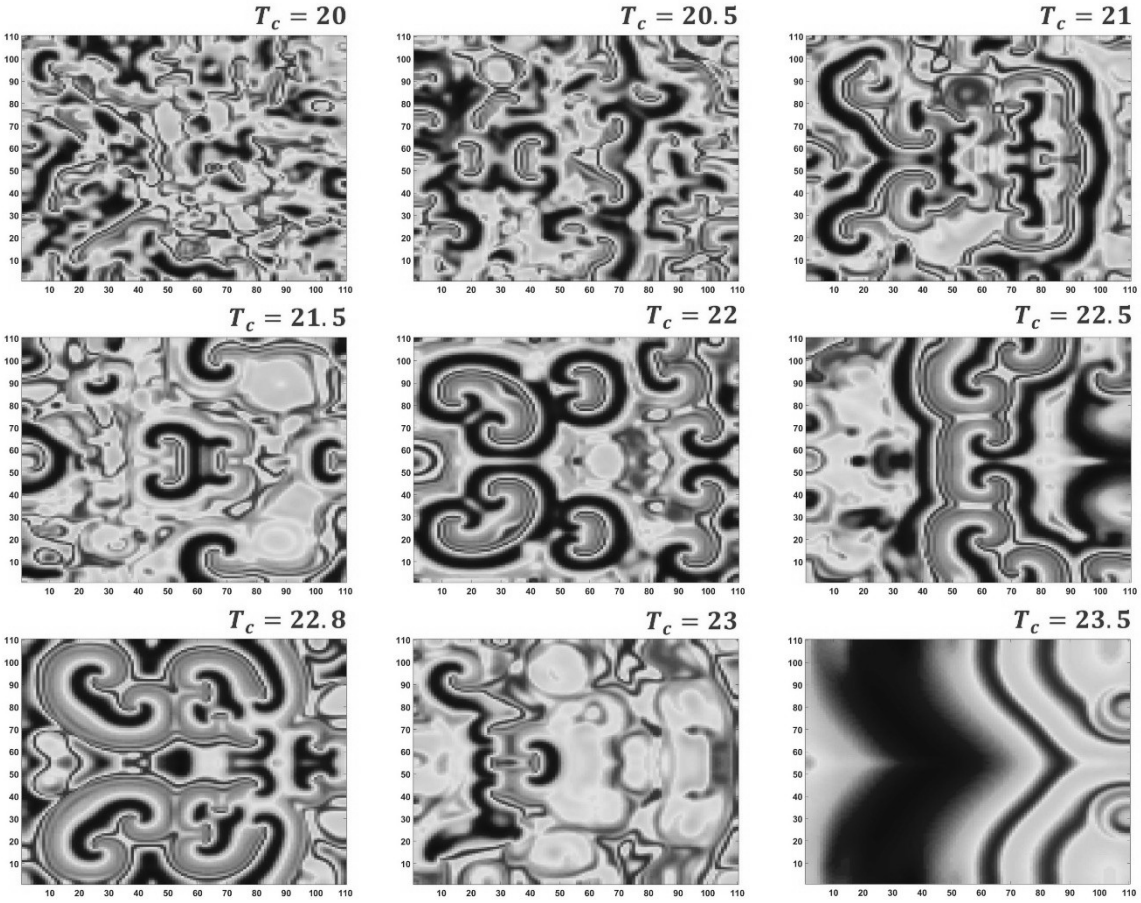

Fig.12: Network snapshots considering temperature affected leaky current in TDML model with electromagnetic field coupling

5. Network dynamics of a multilayer network:

To further enhance our investigation, we expand our discussion to a multilayer lattice network constructed with TDML nodes with different temperature affected channels. The first, second and third layers are constructed considering the lattice network whose nodes are with TDML considering temperature sensitive calcium ion channels, potassium ion channels and temperature affected leaky current channels respectively. The entire discussion is arranged in to two subsections. In the first section we have considered the three layer network with each layer having temperature effects in different ionic channels. In the second subsection only one of the layers is considered to have temperature effect while the other two are considered to have no temperature effects.

5.1 Temperature effects in all three layers:

Fig.13 shows an illustrative construction of the three-layer network. We have assumed the coupling between layers as shown in the Fig.13. The first and the third layers have their coupling with the sandwich layer whereas the sandwich layer will have coupling with both first and third thus making the second layer to have multiple coupling terms. This is the reason we choose the second layer to be the highly temperature sensitive potassium channels as the potassium channels opens secondary channels [32] for certain values of temperatures

and thus have complex behaviors when in a network. The mathematical model of the three-layer network is defined in (6).

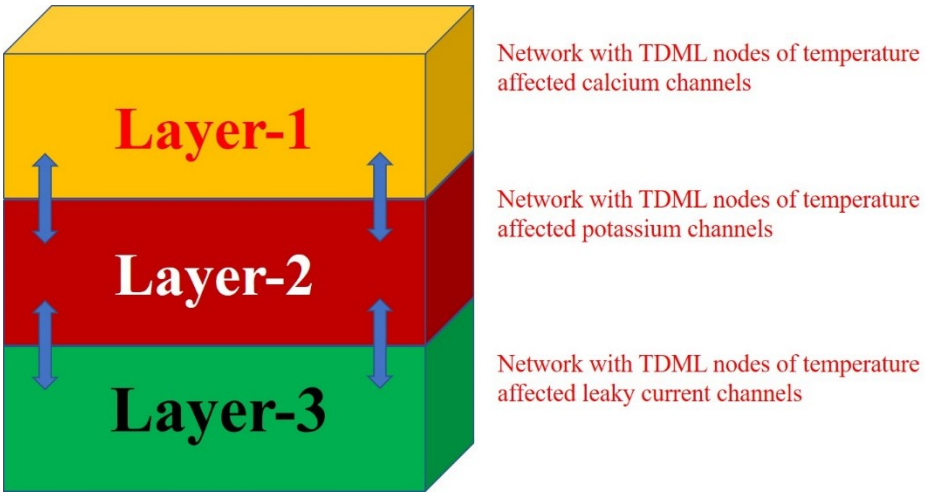

Fig.13: Three-layer network with different temperature sensitive channels of TDML model. The blue bidirectional arrows show the inter layer coupling of the networks. This figure is used just to show the coupling between layers and the thickness of the layers doesn't have any physical meaning as each layer is a lattice network.

Layer-1: Temperature sensitive Calcium ion channel

$$\dot{V}_{1,ij}=g_{CaT}M_{1,\infty}\left(V_{Ca}-V_{1,ij}\right)+g_{KT}W\left(V_K-V_{1,ij}\right)+g_{¿}\left(V_L-V_{1,ij}\right)-I_{1,ij}-k_0M\left(\phi_{1,ij}\right)V$$

$$\dot{W}_{1,ij}=\tau_{1,WT}\left(W_{1,\infty}-W_{1,ij}\right)\dot{I}_{1,ij}=\varepsilon\left(V_0+V_{1,ij}\right)\dot{\phi}_{1,ij}=k_1V_{1,ij}-k_2\phi_{1,ij}$$

Layer-3: Temperature sensitive leak current channel

$$\dot{V}_{3,ij}=g_{CaT}M_{3,\infty}\left(V_{Ca}-V_{3,ij}\right)+g_{KT}W\left(V_K-V_{3,ij}\right)+g_{¿}\left(V_L-V_{3,ij}\right)-I_{3,ij}-k_0M\left(\phi_{3,ij}\right)V$$

$$\dot{W}_{3,ij}=\tau_{3,WT}\left(W_{3,\infty}-W_{3,ij}\right)\dot{I}_{3,ij}=\varepsilon\left(V_0+V_{3,ij}\right)\dot{\phi}_{3,ij}=k_1V_{3,ij}-k_2\phi_{3,ij}$$

Layer-2: Temperature sensitive potassium channel

$$\dot{V}_{2,ij}=g_{CaT}M_{2,\infty}\left(V_{Ca}-V_{2,ij}\right)+g_{KT}W\left(V_K-V_{2,ij}\right)+g_{¿}\left(V_L-V_{2,ij}\right)-I_{2,ij}-k_0M\left(\phi_{2,ij}\right)V$$

$$\dot{W}_{2,ij}=\tau_{2,WT}\left(W_{2,\infty}-W_{2,ij}\right)\dot{I}_{2,ij}=\varepsilon\left(V_0+V_{2,ij}\right)\dot{\phi}_{2,ij}=k_1V_{2,ij}-k_2\phi_{2,ij}$$

(6)

where $F_p\left(V_{p,ij}\right)=D_{p,1}\left(V_{p,i+1\,j}+V_{p,i-1\,j}+V_{p,ij+1}+V_{p,ij-1}-4V_{p,ij}\right)$ which is the intra layer coupling with $p\in(1,2,3)$for the respective layers. The parameter and the stimuli settings are similar to the previous section and we have used the temperature sensitivity coefficients as in Table-1.In the investigations we have fixed the intra layer coupling strength as $D_{p,1}=1, p\in(1,2,3)$ and have considered the current temperature (T_c), the inter layer coupling strength $D_{IL_p}, \in p(1,2,3)$ and flux coupling coefficient (k_0) as the control

parameters. We have considered two scenarios for discussion viz without electromagnetic flux coupling and with electromagnetic flux coupling.

Table-1: Temperature sensitivity coefficients for the three-layer network

Layers	Q_{Ca}	Q_K	Q_L	Q_w
1	3	1	1	1
2	1	3	1	1
3	1	1	3	1

In the first scenario we have considered the three-layer TDML network (6) without magnetic flux coupling and thus the TDML model reduces from 4D to a 3D system. In order to induce spiral waves in all three layers, we have considered the initial condition setup for selected nodes are given in Table-2 while the initial conditions of the other nodes are kept as [0,0,0]. It is to be noted that the same initial condition setup is applied in all the three layers.

Table-2: Initial conditions setup for the nodes $[i, j]$ in the network (6)

$[i, j]$	V_0	W_0	I_0
25:50,40:45	0.1	-0.1	-0.05
25:50,55:60	-0.05	-0.07	0.1
25:50,70:80	0.5	0.1	-0.3

For the discussion, we have considered the current temperature (T_c) and the inter layer coupling$D_{IL_p}=D, \in p(1,2,3)$. The required system parameters for the TDML model are derived as in [23] and the stimuli parameters are same as in previous section. With these settings and considering no flux boundary conditions, we have captured the spatiotemporal dynamics of the three-layer network. In the first analysis we have considered the three-layer network whose local nodes are the TDML neurons without flux coupling. The current temperature (T_c) is considered the control parameter and the snapshots are shown in Fig.14. It was shown earlier that the temperature affected calcium channel models (case-a) show spiral turbulence for values of $T_c>21.5$ but in the three layer network the spiral waves are seen in layer-1 (case-a) for temperature $T_c=20.5$ and this is because of the interference from the other layers which show spiral seeds for lesser temperatures. Even the layers are seen synchronized for the temperature ranges $20.5\leq T_c\leq 22.8$ and for $T_c=21.8$, a completely synchronized spiral wave pattern with nearly similar amplitude and angular characteristics is

seen. But when T_c=22 all the three layers dissipate the spiral seeds which was not the case when we analyzed the layers separately. This is because the networks enter perfect synchronization and chaotic spiking nodes enters into periodic spiking due to the coupling between the networks introducing order in the nodes.

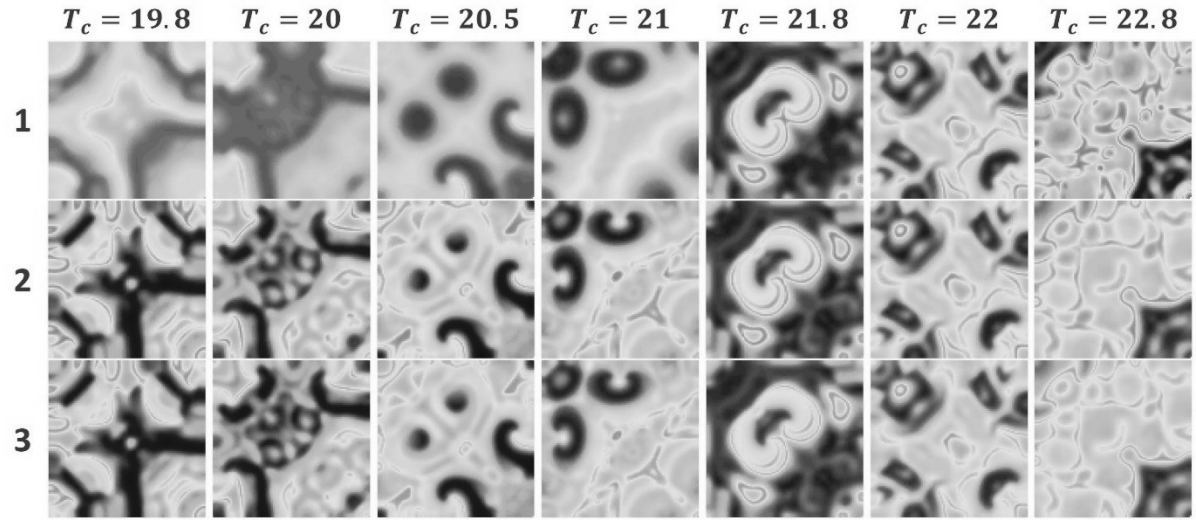

Fig.14: The spatiotemporal dynamics of the three-layer network captured for 1000s considering the TDML nodes without electromagnetic flux coupling

Int second discussion on the three-layer network without electromagnetic flux coupling, we consider the inter layer coupling strength D as the control parameter and study the spatiotemporal dynamics by fixing T_c=21.8 . As shown in Fig.15, when the coupling strength is low, there is no spiral waves seen in all the three layers which confirms that the coupling strength plays a major role in spiral wave turbulence. Increasing the coupling strength to 0.01, layer-2 and layer-3 shows multiple rotating spirals whereas layer-1 shows induced spiral seeds with much lesser frequency of rotation. This is because of the TDML nodes behaving in a anti synchronized pattern with layer-2. But when D=0.05 all three layers are in compete synchronization thus showing spiral wave with similar characters. But when coupling is increased further the spiral waves breaks into multiple small amplitude spiral seeds which are then dissipated in the network.

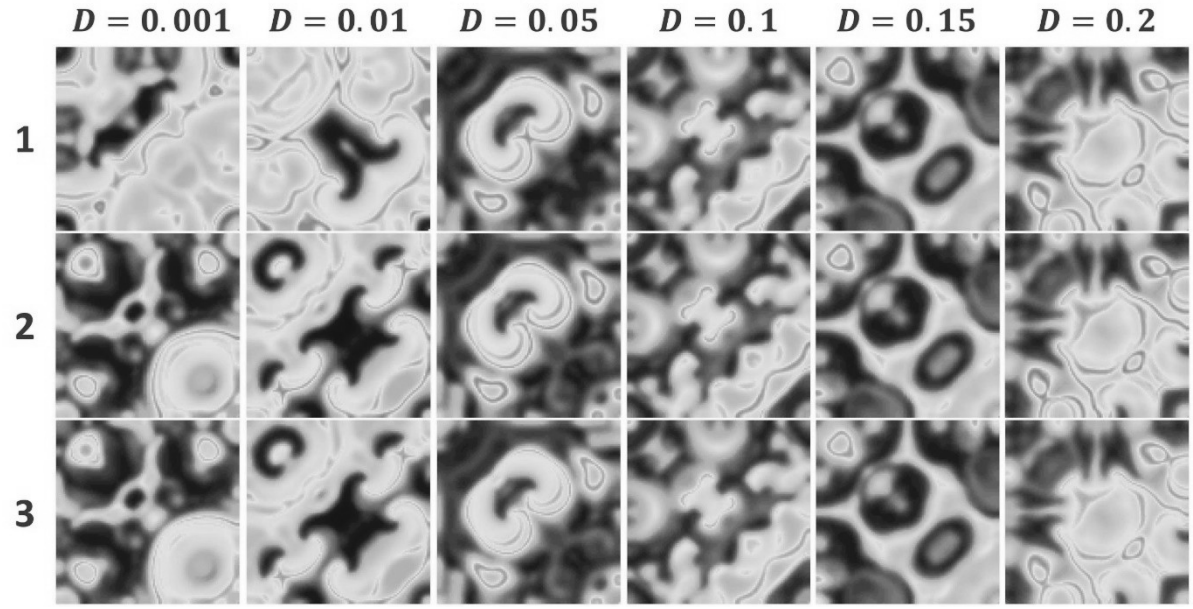

Fig.15: Effect of inter layer coupling strength on the spatiotemporal dynamics of the three-layer network captured for 1000s considering the TDML nodes without electromagnetic flux coupling

Showing that the three-layer network considered without flux coupling exhibits spiral waves only for a smaller range of T_c, our interest I to see the effect of flux coupling on the network behavior. It could be easily seen from Fig.16, that the network shows spiral waves in all three layers for a much wider temperature range. To be exact the spiral seeds are seen in all three layers for a much lesser temperature value T_c=19.5 and was seen till T_c=23. Another aspect to note is that all three layers behave in a much-synchronized pattern and this is because of the flux coupling considered for the local nodes in each layer. This local flux coupling increases the coupling strength between the inter layer neurons due to the considered feedback coupling.

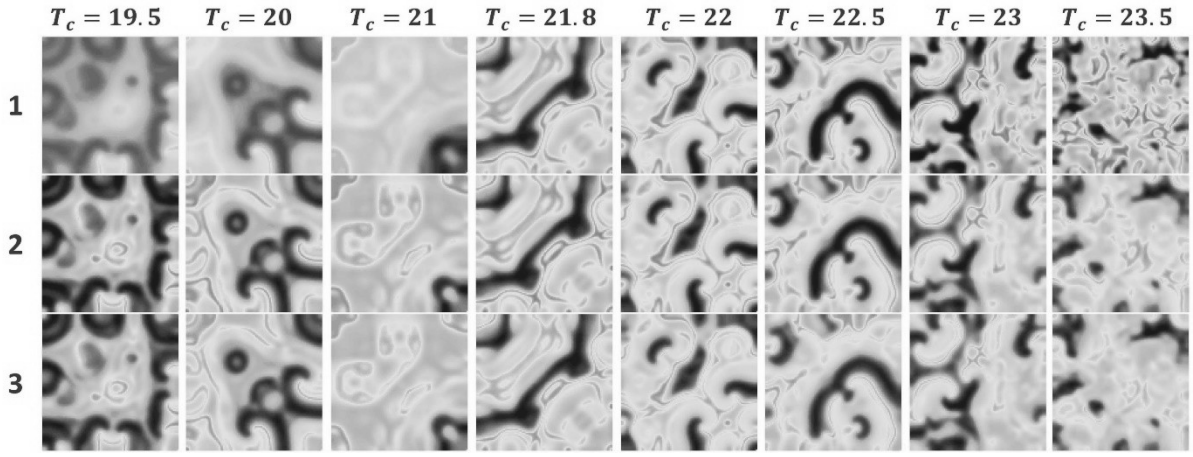

Fig.16: The spatiotemporal dynamics of the three-layer network captured for 1000s considering the TDML nodes with electromagnetic flux coupling

To show that the flux coupling indirectly increase the coupling strength between layers, we now consider the inter layer coupling strength as the control parameter as shown in Fig.17. In Fig.18 we could see that for D=0.001 there is no spiral waves seen in layer-1 whereas all three layers show spiral seeds in Fig.20. This is because of the local flux coupling in the nodes which extends for the entire coupling strength $0.001 \leq D \leq 0.2$ with all three layers behaving in complete synchronization.

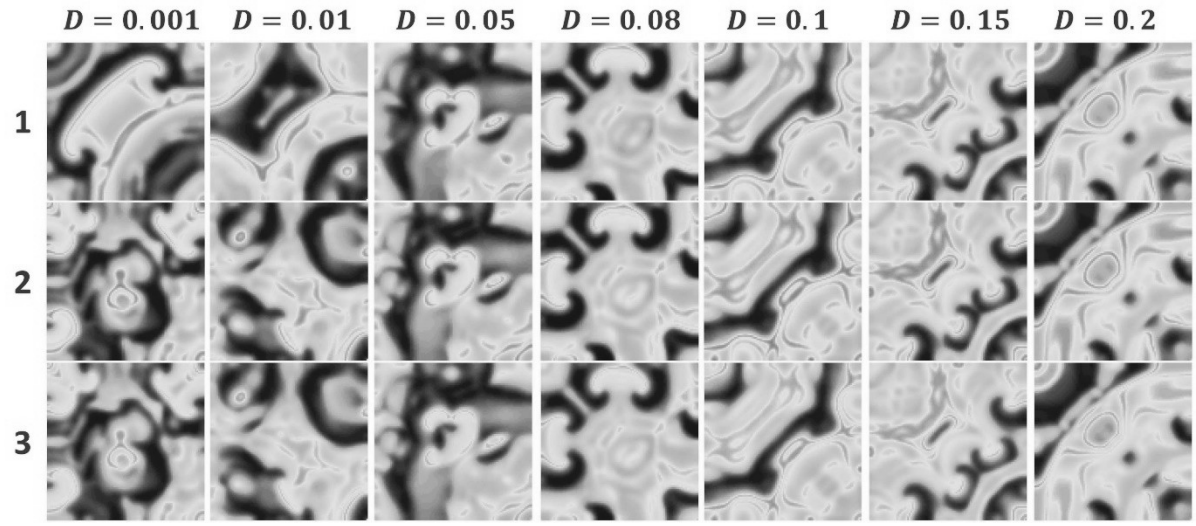

Fig.17: Effect of inter layer coupling strength on the spatiotemporal dynamics of the three-layer network captured for 1000s considering the TDML nodes with electromagnetic flux coupling

5.2 Temperature effect considered in one of the layers:

For the investigation of temperature effects in one of the layers, we consider three different scenarios. In the first scenario the temperature effects is considered in all the three ion channels in the first layer while the second and third layer is considered to have no temperature effects. In the second and third scenario the respective second and third layers are considered to have temperature affected ion channels while the other channels don't have temperature effects. The inter layer coupling strength are kept at $D=0.1$ and the stimuli parameters are same as in previous section. It should be noted that the parameter and coupling strengths are kept to the values where the layer behaves synchronously. These setting are defined in the previous section while the inter layer coupling strength is selected from the analysis presented in section 5.1.

For the first scenario we have introduced temperature effects in all the three channels (calcium, potassium and leaky current) of the first neuron layer while the other two layers don't have temperature affected ion channels. It should be noted that for this analysis we have considered no flux effects. For temperature values $T_c<21.5$, the first layer goes unstable and thus driving the other two layers also to instability. The wave propagation is seen when the temperature raises to $T_c=21.5$ but no sign of spiral turbulence. When $T_c=22$, the first layer is similar to other two layers with no temperature effects and shows the initiation of spiral waves. This can be corroborated with Fig.7 which shows the same behavior of spiral waves

for $21.8 \leq T_c \leq 22.5$ very similar to Fig.18. Since the other two layers are given the parameter setting of chaotic spiking ($T_c = 22$), we expected the networks to show turbulent spiral waves. But due to strong synchrony existence between the layers, the second and third layers also show similar non-spiral wave patterns as like the first layer for $T_c = 21.5 \wedge 24$.

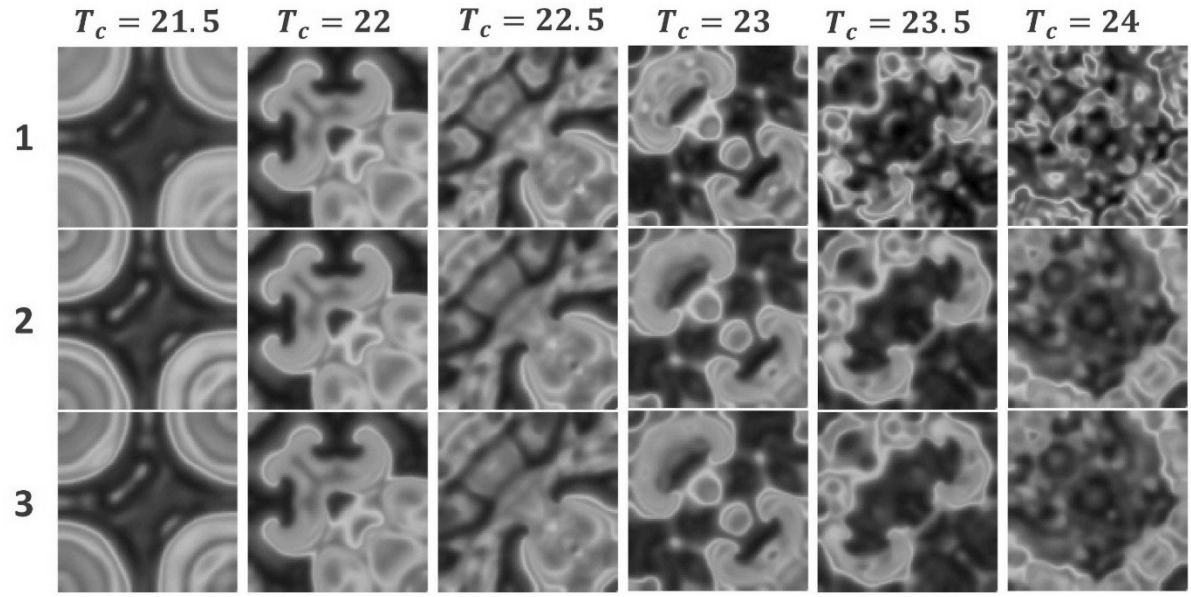

Fig.18: Captured network dynamics of the three-layer network considering temperature effects in the first neuron layer while the other two neuron layers have no temperature effects. The nodes are considered to have no flux effects.

To understand the effect of magnetic flux on the network, we now include the flux coupling to the nodes in the network. Fig.19 shows the spatiotemporal dynamics of the three-layer network considering the flux effects on the nodes. Comparing Fig.18 with Fig.19, we could see that the range of temperature for which the network shows spiral waves have extended to $T_c = 25$ and the network goes unstable after this temperature. Also, for $T_c = 22.5$ we could see that the spiral waves are suppressed by the flux effect but reemerges for $T_c = 23$. We could also see that all the three layers remain in complete synchrony for all the temperatures like Fig.18. This could confirm that the effect of flux on the nodes is very little and doesn't change the behavior of the networks as a whole.

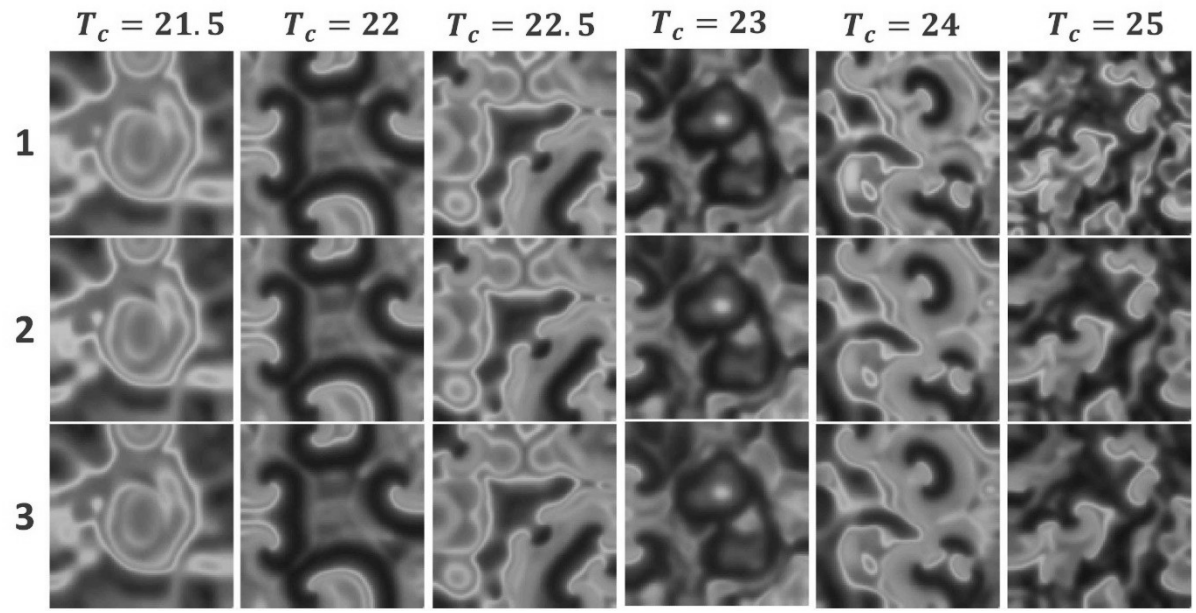

Fig.19: Captured network dynamics of the three-layer network considering temperature effects in the first neuron layer while the other two neuron layers have no temperature effects. The nodes are considered to have magnetic flux effects.

In the second scenario, we consider the temperature effects on ion channels in second layer while the first- and third-layer nodes are considered without such temperature effects. Fig.20 shows the spatiotemporal snapshots of the network considering that the nodes in all the three layers are without flux linkage and the second layer alone has temperature effects. All the three network remains in complete synchrony and the spiral waves are seen in the network for a very narrow temperate range of $21.5 \leq T_c \leq 23$ and the wave propagation is completely suppressed and the network remains in near idle state for $23.5 \leq T_c \leq 24$ and after this range the network goes unstable. As the second layer is coupled with both first and third layers, the dynamic changes happening in second layer affects the other layers immediately and hence the wave propagation is suppressed in first and third layer as soon as it happens in second layer. This cannot be seen in Fig.18 as the wave propagation extended till $T_c = 24$.

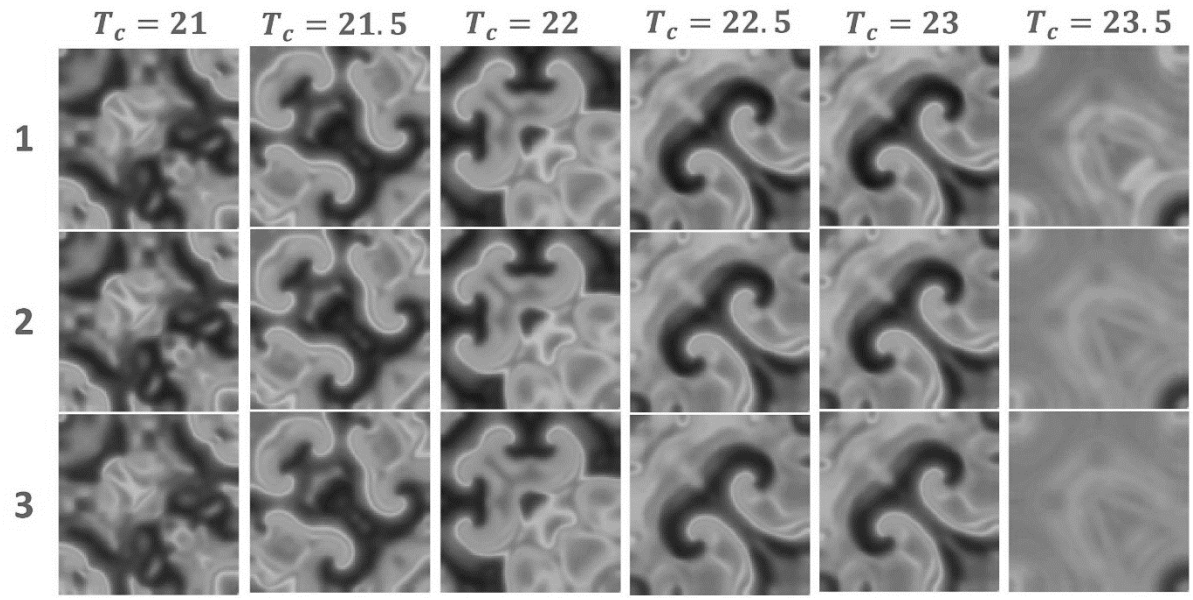

Fig.20: Captured network dynamics of the three-layer network considering temperature effects in the second neuron layer while the other two neuron layers have no temperature effects. The nodes are considered to have no flux effects.

In Fig.21, we consider that the nodes in the network are exposed to magnetic flux effects and we consider second layer to have temperature affected ion channels. Comparing Fig.20 and Fig.21, we could see that the nodes exposed to magnetic flux will exhibit spiral wave phenomenon for $T_c > 23$ which was not seen in Fig.21 where the network has no sign of spiral turbulence for $T_c > 23$. This is because that the flux coupling in the nodes extends the bursting regime of them and hence will facilitate the propagation of spiral waves for a broader temperature range. For $T_c = 27$, the synchrony between the first with the other layers is seen broken as the first layer nodes are in complete asynchronous state and no more supports wave propagation. The second and the third layer are seen in synchronous behavior with one another. Further increase in temperature will result in all the layers to go unstable.

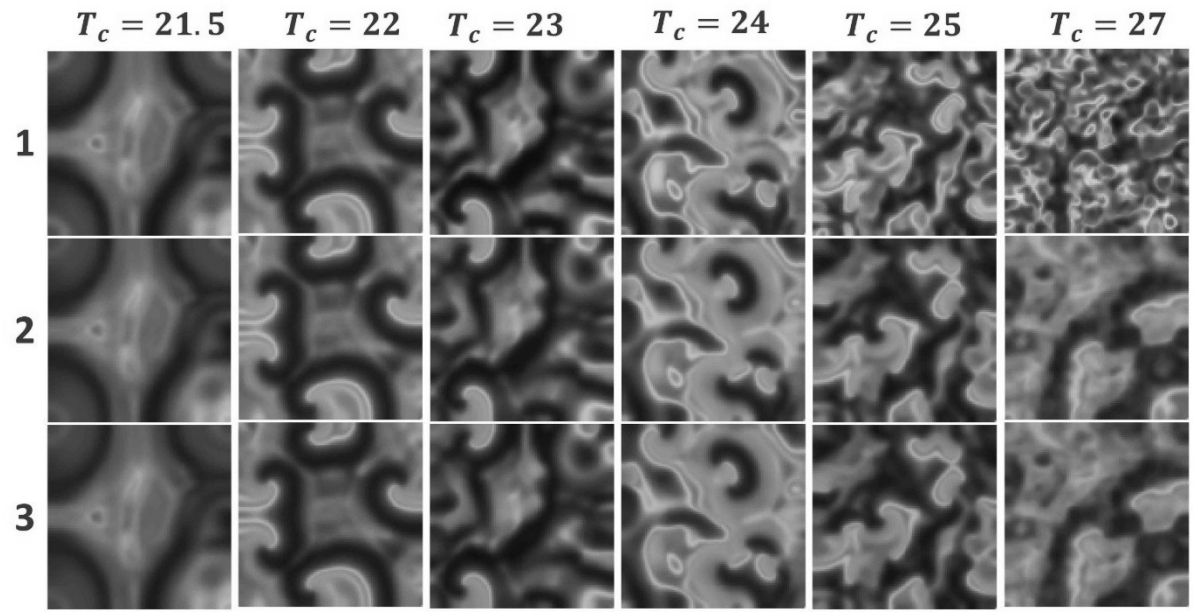

Fig.21: Captured network dynamics of the three-layer network considering temperature effects in the second neuron layer while the other two neuron layers have no temperature effects. The nodes are considered to have flux effects.

In the final scenario, we consider that the nodes in the third layer consists of temperature affected ion channels while the first- and second-layer nodes have no temperature effects. We have also considered that the nodes in all the three layers have no flux effects. Fig.22 shows the network snapshots for different temperature values. The network shows spiral waves for temperature ranges as low as T_c=17 and shows the spiral waves with the same character till T_c=35. All the three layers behave in complete coherency and never showed even a lag in spiral phenomenon. Further increasing the temperature to T_c>35, the network goes unstable and no more support wave propagation. We could conclude from this inference that the third layer has a much lesser impact on the network compared to the other two layers and the collective behavior and coherency between the three layers are considered to be high in this case as against the other two scenarios.

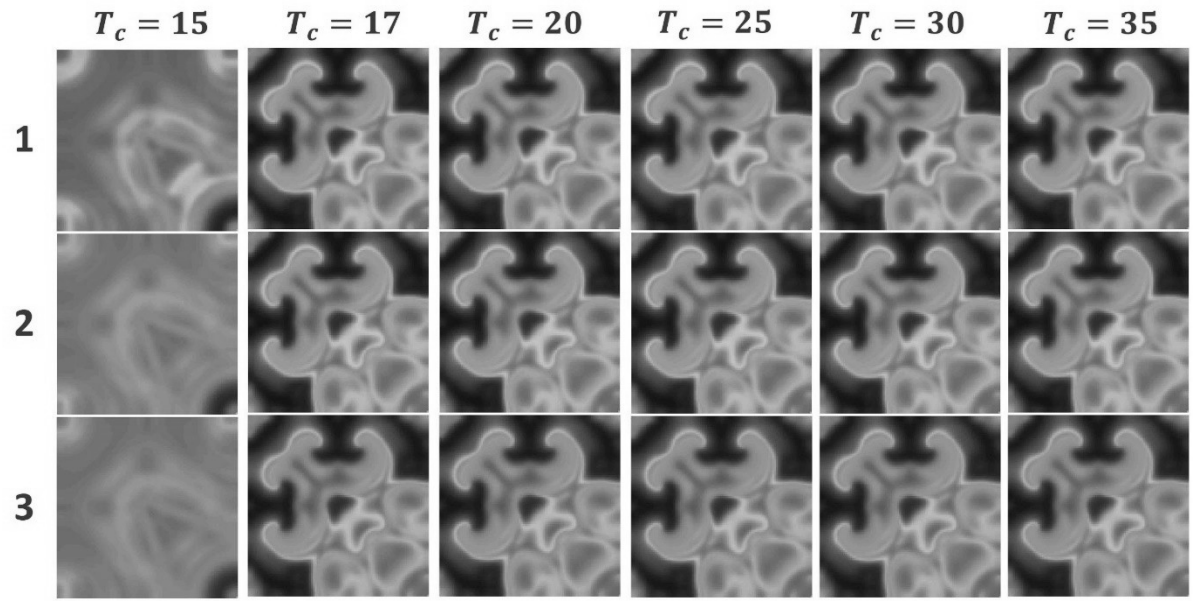

Fig.22: Captured network dynamics of the three-layer network considering temperature effects in the third neuron layer while the other two neuron layers have no temperature effects. The nodes are considered to have no flux effects.

As we have shown in Fig.22, the temperature effects in the third layer will not have significant effect on the spiral wave turbulence we now focus on studying the effect of flux effects on the nodes in all the layers. Fig.23 shows the spatiotemporal dynamics of the network behavior and the network is not much affected by the flux coupling and the spiral waves are seen for the same range of temperature as in Fig.22. The entire network goes unstable for T_c>35 and varying the flux coupling strength k_0 will not much affect this behavior of the layers.

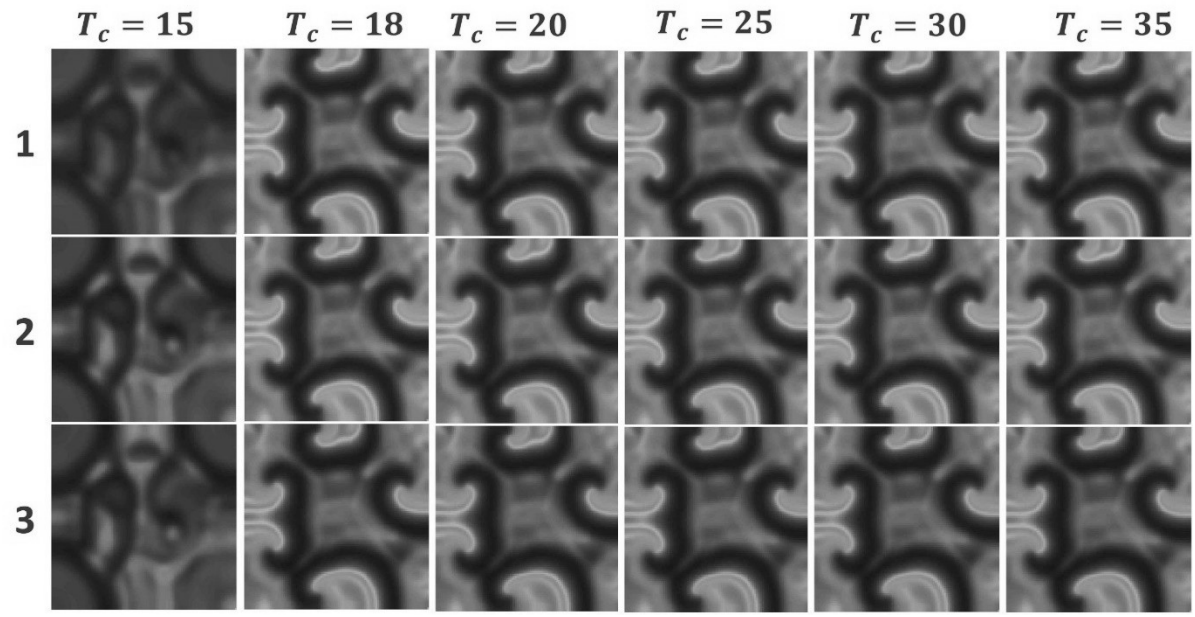

Fig.23: Captured network dynamics of the three-layer network considering temperature effects in the third neuron layer while the other two neuron layers have no temperature effects. The nodes are considered to have flux effects.

6. Results and Discussion

We have investigated the temperature effects on the well-known ML neuron model and have presented the various dynamical properties of the model considering the current temperature as the control parameter. When mentioning temperature effects, we considered temperature affected calcium, potassium and leak current channels separately and the temperature effects on these channels are investigated. We could show that calcium channels reaction to temperature is very narrow compared to the potassium channels and leak current channels. Specifically, the bifurcation of the TDML model with current temperature shows that the calcium channels have a much narrow chaotic range while the temperature effects of potassium and leak current have a wider range. The Lyapunov spectrum presented confirm the bifurcation ranges and also the Hopf's bifurcation points presented correlate with the bifurcation diagrams.

After investigating the local dynamical effects of temperature on the ML model, we constructed two type of networks to understand the collective behavior. In the first type, a simple 2D lattice network with TDML neurons is constructed considering no flux boundary and a periodical stimulus applied to the left boundary of the network. In this discussion we have considered three different cases for temperature affected calcium, potassium and leak current channels and in each case, we have considered two scenarios with the first scenario for TDML model without magnetic coupling and in the second scenario with magnetic coupling. This discussion will help us to understand the influence of flux coupling on the wave propagation. In the first case considering temperature affected calcium channels, the magnetic field coupling doesn't create any difference in the wave propagation phenomenon as spiral waves are seen for the temperature regions $21.8 \leq T_c \leq 22.3$ and the network goes

unbounded for $T_c > 22.8$. When the potassium channels are considered, the TDML without flux coupling shows spiral waves for a much wider range $19.5 \le T_c \le 23.3$ whereas when we consider the flux coupling the spiral wave range reduce to $19.5 \le T_c \le 22.5$. But when we tried increasing the flux coupling strength to understand whether the controlling behavior of the flux coupling on spiral waves, we noted that increasing the coupling strength will drive the network unbounded. Similar was not the case when we considered temperature affected leaky current channels where we could note the spiral waves for both with and without flux coupling where the range is $20 \le T_c \le 23.2$. Thus, we could conclude that the flux coupling effects on all the three cases are not much commendable as the spiral waves are seen in both the scenarios.

In the second type of network, we constructed a three-layer network with each layer having three different lattice layers. The investigation is divided in to two scenarios. In the first, the three lattice layers are constructed with first, second and third layers having temperature affected calcium, potassium and leak current channels respectively. The stimulus setting are taken as in the single layer network analysis and we have considered a different set of initial conditions for certain nodes in the network. The inter layer coupling and the current temperature are considered as the control parameters for discussion. Again, we have considered two scenarios with first considering TDML model without flux coupling while the second being with flux coupling. The wave propagation in the first scenario shows that all three layers have shown spiral waves in a much-synchronized pattern $19.8 \le T_c \le 22.8$ while actually potassium channels have shown spiral waves for values of temperature $T_c > 22.8$. This shows that the inter layer coupling affects the spiral waves in the layers and thus one layers wave propagation pattern affects the other. While we considered the flux coupling, the synchronized spiral waves in the three layers are seen $19.5 \le T_c \le 23.5$ and this time we could see that the potassium channels now affects the other two channels and influencing spiral waves in the other layers (mainly the calcium affected TDML) as when considered the calcium affected TDML model alone the spiral waves won't last over temperature of 22.5. The effects of inter layer coupling for both scenarios are also presented where we have shown that the three layers are synchronized even for lower coupling strengths of 0.001. In the scenario considering flux coupling in all the three layers, we could note that the spiral waves exist for a much wider coupling range ($0.001 \le D \le 0.2$) while the range is much lesser when flux coupling is not considered ($0.001 \le D \le 0.1$¿.

In the second scenario of the multilayer spatiotemporal investigation we have now considered only one layer to have temperature effect in all the three channels while the other layers are considered to have no temperature effects on their ion and leaky current channels. Through this investigation we would like to study about the network behavior when only one layer is exposed to temperature. For the first case we have introduced temperature effects in all the three channels (calcium, potassium and leaky current) of the first neuron layer while the other two layers don't have temperature affected ion channels. When the layers are considered without flux effects, the spiral waves are seen for a much smaller range of temperature $T_c = 22$¿23.5. whereas when exposed to flux effects the range extends to $22 \le T_c \le 25$. This is because that the flux coupling extends the chaotic region of the neuron nodes. In the second

case we consider that the intermediate layer is have temperature affected ion channels and when this network is considered to have no flux effects the network shows spiral waves for $21 \le T_c \le 23$ whereas when exposed to flux effects the network will have spiral waves for $22 \le T_c \le 25$. Again this range increase is because of the chaotic spiking of the nodes for a much broader temperature range when exposed to flux effects. In the final discussion we consider the third layer to have the temperature effects. We could notice that all the three layers behave synchronously for a very wide temperature range showing spiral waves with much stable behavior. The range of temperature is $17 \le T_c \le 35$ for which the spiral wave turbulence if noted in the network. This range is not affected by the flux coupling and after $T_c = 35$, the entire network goes unstable. Hence, we could say that the third layer has minimum effect of temperature on the network whereas the first layer has the maximum temperature effect.

Reference:

[1]. Eugene M. Izhikevich, "Which Model to Use for Cortical Spiking Neurons?", IEEE Transactions On Neural Networks, Vol. 15, No. 5, 2004.

[2]. Mengyan Ge, Ya Jia, Ying Xu, Lijian Yang, "Mode transition in electrical activities of neuron driven by high and low frequency stimulus in the presence of electromagnetic induction and radiation", Nonlinear Dyn, Springer Science+Business Media B.V, 2017 DOI 10.1007/s11071-017-3886-2

[3]. Jasmina Isakovic, Ian Dobbs-Dixon, Dipesh Chaudhury, Dinko Mitrecic, "Modeling of inhomogeneous electromagnetic fields in the nervous system: a novel paradigm in understanding cell interactions, disease etiology and therapy", Scientific Reports, (2018) 8:12909 | DOI:10.1038/s41598-018-31054-9

[4]. Yanbing Jia, Bo Lu, Huaguang Gu, "Excitatory electromagnetic induction current enhances coherence resonance of the FitzHugh Nagumo neuron", International Journal of Modern Physics B, World Scientific Publishing Company, Vol. 33 (2019) 1950242 (13 pages) DOI: 10.1142/S0217979219502424

[5]. Tingting Fang, Jiqian Zhang, Shoufang Huang, Fei Xu, Maosheng Wang, Hang Yang, "Synchronous behavior among different regions of the neural system induced by electromagnetic radiation", Nonlinear Dyn, Springer Nature B.V. 2019. DOI:10.1007/s11071-019-05260-7

[6]. Zhan F, Liu S "Response of Electrical Activity in an Improved Neuron Model under Electromagnetic Radiation and Noise", Front. Comput. Neurosci. 11:107, (2017)

[7]. Iftinca M, McKay BE, Snutch TP, McRory JE, Turner RW, Zamponi GW. Temperature dependence of T-type calcium channel gating. Neuroscience. 2006; 142: 1031–1042. https://doi.org/10.1016/j. neuroscience.2006.07.010 PMID: 16935432

[8]. Coulter DA, Huguenard JR, Prince DA. "Calcium currents in rat thalamocortical relay neurones: kinetic properties of the transient, low-threshold current". J Physiol. 1989; 414: 587–604. https://doi.org/10.1113/jphysiol.1989.sp017705 PMID: 2607443

[9]. Yang F, Zheng J. “High temperature sensitivity is intrinsic to voltage-gated potassium channels”. eLife.2014; 3: e03255. https://doi.org/10.7554/eLife.03255 PMID: 25030910
[10]. Van Hook MJ (2020) “Temperature effects on synaptic transmission and neuronal function in the visual thalamus. PLoS ONE 15(4): e0232451.
[11]. Lulu Lu, John Billy Kirunda, Ying Xu, Wenjing Kang, Run Ye, Xuan Zhan, and Ya Jia “Effects of temperature and electromagnetic induction on action potential of Hodgkin-Huxley model” Eur. Phys. J. Special Topics 227, 767-776 (2018)
[12]. Guo D Q, Chen M, Perc M, et al. “Firing regulation of fast-spiking interneurons by autaptic inhibition”. EPL, 2016, 114: 30001
[13]. Guo D Q, Wu S, Chen M, et al. “Regulation of irregular neuronal firing by autaptic transmission”. Sci Rep, 2016, 6: 26096
[14]. Qin H X, Wu Y, Wang C N, et al. “Emitting waves from defects in network with autapses”, Commun Nonlinear Sci Numer Simul, 2015, 23: 164–174
[15]. Ma J, Qin H X, Song X L, et al. “Pattern selection in neuronal network driven by electric autapses with diversity in time delays”, Int J Mod Phys B, 2015, 29: 1450239
[16]. Qin H X, Ma J, Wang C N, et al. “Autapse-induced target wave, spiral wave in regular network of neurons”, Sci China-Phys Mech Astron, 2014, 57: 1918–1926
[17]. Xing, M., Song, X., Yang, Z. et al. “Bifurcations and excitability in the temperature-sensitive Morris–Lecar neuron”. Nonlinear Dyn 100, 2687–2698 (2020). https://doi.org/10.1007/s11071-020-05667-7.
[18]. Morris, C., Lecar, H.: “Voltage oscillations in the barnacle giant muscle fiber”. Biophys. J. 35(1), 193–213 (1981).
[19]. Lv M , Ma J . “Multiple modes of electrical activities in a new neuron model under electromagnetic radiation”, Neurocomput 2016, 205:3, 75–81, 2016.
[20]. Karthikeyan Rajagopal, Fahimeh Nazarimehr, Anitha Karthikeyan, Ahmed Alsaedi, Tasawar Hayat, Viet-Thanh Pham, “Dynamics of a neuron exposed to integer order and fractional order discontinuous external magnetic flux”, Frontiers of Information Technology & Electronic Engineering, (2019) 20: 584. 2019. https://doi.org/10.1631/FITEE.1800389.
[21]. Karthikeyan Rajagopal, Abdul Jalil M. Khalaf, Fatemeh Parastesh, Irene Moroz, Anitha Karthikeyan, Sajad Jafari, “Dynamical behavior and network analysis of an extended Hindmarsh–Rose neuron model”, Nonlinear Dyn (2019) 98: 477, 2019. https://doi.org/10.1007/s11071-019-05205-0.
[22]. Jun Ma, Fuqiang Wu, Chunni Wang, “Synchronization behaviors of coupled neurons under electromagnetic radiation”, International Journal of Modern Physics B, World Scientific Publishing Company, Vol. 31, No. 2 (2017) 1650251 (14 pages).
[23]. Rajagopal, K., Moroz, I., Karthikeyan, A. et al. “Wave propagation in a network of extended Morris–Lecar neurons with electromagnetic induction and its local kinetics”, Nonlinear Dyn (2020). https://doi.org/10.1007/s11071-020-05643-1.
[24]. FuQiang Wu, Jun Ma, Ge Zhang "Energy estimation and coupling synchronization between biophysical neurons" Science China Technological Sciences, 2019.

[25]. Panfilov A.V. (2019) “Spiral Waves in the Heart”. In: Tsuji K., Müller S. (eds) Spirals and Vortices. The Frontiers Collection. Springer, Cham, https://doi.org/10.1007/978-3-030-05798-5_11.
[26]. Garfinkel, A., Kim, Y.H., Voroshilovsky, O., Qu, Z., Kil, J.R., Lee, M.H., Karagueuzian, H.S., Weiss, J.N., Chen, P.S.: “Preventing ventricular fibrillation by flattening cardiac restitution”. Proc. Natl. Acad. Sci. USA 97, 6061 (2000).
[27]. Davidenko, J.M., Pertsov, A.V., Salomonsz, R., Baxter, W., Jalife, J.: “Stationary and drifting spiral waves of excitation in isolated cardiac muscle”. Nature 355, 349–351 (1992)
[28]. Karthikeyan Rajagopal, Fatemeh Parastesh, Hamed Azarnoush, Boshra Hatef, Sajad Jafari and Vesna Berec, "Spiral waves in externally excited neuronal network: solvable model with a monotonically differentiable magnetic flux", Chaos: An Interdisciplinary Journal of Nonlinear Science. 2019.
[29]. Karthikeyan Rajagopal, Abdul Jalil M. Khalaf, Fatemeh Parastesh, Irene Moroz, Anitha Karthikeyan, Sajad Jafari, “Dynamical behavior and network analysis of an extended Hindmarsh–Rose neuron model”, Nonlinear Dyn (2019) 98: 477, 2019. https://doi.org/10.1007/s11071-019-05205-0.
[30]. Jun Ma, Ya Wang, Chunni Wang, Ying Xu, Guodong Ren, “Mode selection in electrical activities of myocardial cell exposed to electromagnetic radiation”, Chaos, Solitons and Fractals 99 (2017) 219–225, 2017.
[31]. Sarria, I., Ling, J., & Gu, J. G. (2012). “Thermal sensitivity of voltage-gated Na+ channels and A-type K+ channels contributes to somatosensory neuron excitability at cooling temperatures”, Journal of neurochemistry, 122(6), 1145–1154. https://doi.org/10.1111/j.1471-4159.2012.07839.x
[32]. S C Lee and C Deutsch, “Temperature dependence of K(+)-channel properties in human T lymphocytes”, Biophys J. 1990 Jan; 57(1): 49–62.
[33]. Rostami, Z., Jafari, S., Perc, M. et al. “Elimination of spiral waves in excitable media by magnetic induction”, Nonlinear Dyn 94, 679–692 (2018). https://doi.org/10.1007/s11071-018-4385-9.
[34]. A. Wolf, J. B. Swift, H. L. Swinney, J. A. Vastano, "Determining Lyapunov exponents from a time series," Physica D: Nonlinear Phenomena, . 16, 285-317, (1985).